

RSC Advances



This is an *Accepted Manuscript*, which has been through the Royal Society of Chemistry peer review process and has been accepted for publication.

Accepted Manuscripts are published online shortly after acceptance, before technical editing, formatting and proof reading. Using this free service, authors can make their results available to the community, in citable form, before we publish the edited article. This *Accepted Manuscript* will be replaced by the edited, formatted and paginated article as soon as this is available.

You can find more information about *Accepted Manuscripts* in the [Information for Authors](#).

Please note that technical editing may introduce minor changes to the text and/or graphics, which may alter content. The journal's standard [Terms & Conditions](#) and the [Ethical guidelines](#) still apply. In no event shall the Royal Society of Chemistry be held responsible for any errors or omissions in this *Accepted Manuscript* or any consequences arising from the use of any information it contains.

COMMUNICATION

Cite this: DOI: 10.1039/x0xx00000x

Received 00th January 2012,
Accepted 00th January 2012

DOI: 10.1039/x0xx00000x

www.rsc.org/

Graphene oxide-based electrochemical sensor: A platform for ultrasensitive detection of heavy metal ions

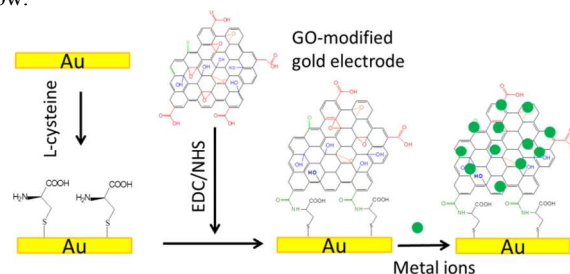
Xuezhong Gong,¹ Yunlong Bi,¹ Yihua Zhao,¹ Guozhen Liu² and Wey Yang Teoh^{*1}

Facile functionalization of graphene oxide sheets on gold surface results in complexation-enhanced electrochemical detection of heavy metal ions, shown here for Pb²⁺, Cu²⁺ and Hg²⁺, with improved detection limits by two order of magnitudes relative to control electrode.

The applications of graphene in Nanotechnology-based devices have received unceasing interests since its discovery, attributing to its unique and often outstanding physicochemical and electronic properties.¹ For electronic devices, extremely high quality graphene with little defects and oxygenated group are necessary, and this is commonly synthesized through very delicate chemical vapor synthesis often with low yield.² As to chemical applications, the trends in the recent years have been focusing on the adaptation of reduced-graphene oxide (rGO), a lower quality variant of graphene analogue, that can be obtained from the chemical reduction of oxidized and exfoliated graphite.³ For even simpler and cheaper processing, graphene oxide (GO) sheets, which are obtained right after the oxidation/exfoliation of graphite without further reduction step, can be explored for various applications such as hybrid functional materials,⁴ drug-delivery vehicles,⁵ and fluorescence-based sensors.⁶ This is despite the much lower electrical conductivity (at least two order of magnitudes) of GO compared to rGO.⁷ Nevertheless, given its large specific surface area and strong hydrophilic nature, GO shows great potential in the removal of aqueous pollutants,⁸ especially for a wide range of heavy metal ions.⁹ For example, the strong interactions of Cu²⁺ with GO surface makes it an excellent adsorbent material,¹⁰ while at the same time also enhances the electronic conductivity through metal ions binding with the oxygen moieties on GO surface.¹¹ In the same way Ca²⁺ and Mg²⁺ can be deliberately added as cross-linkers to enhance the mechanical strength of graphene oxide composites.¹²

Following this train of thoughts, we design GO-based electrochemical sensor on the basis of two important characteristics, that is, high adsorption of analyte and good conductivity thereafter. The GO was synthesized from the oxidation and exfoliation of purified graphite powders, following the well-established Hummers' method¹³ (see ESI[†]). The washed, filtered and dried brownish GO

consists of dense mixed oxygenated groups, such as hydroxyl and epoxide (mostly on the basal surface), and carboxyl (mostly at the sheet edges).¹⁴ These oxygenated moieties provide avenues for direct modification by surface covalent functionalization.^{4,5,15} Using the ethyl(dimethylaminopropyl) carbodiimide / N-hydroxysuccinimide (EDC/NHS) mediated coupling strategy, the edges of GO, that is through carboxyl group, are attached directly onto the L-cysteine modified gold electrode surface (Scheme 1, see ESI for detailed procedures). To the best of knowledge, this is the first report to fabricate the GO-based sensor using the facile EDC/NHS coupling strategy to the ultrasensitive detection of heavy metal ions. The attached GO sheets (see electron microscopy images, Figure S2) form the extended heterogeneous sites for the adsorption of metal ions, predominantly through the oxygenated sites as discussed below.



Scheme 1. Stepwise modification of gold electrode with L-cysteine functionalization followed by the EDC/NHS-mediated coupling of activated GO. The oxygenated sites of attached GO provide avenues for the capturing and complexation of metal ion analytes.

Wide scan X-ray photoelectron spectroscopy (XPS) confirms the presence of Au, S, C, N and O upon self-assembled monolayer attachment of L-cysteine on the bare gold surface (Figure 1a). The carboxyl (O=C–O) and amide (–NH₂) moieties are clearly evident from the C 1s binding energy peaks at 288.8 eV (Figure 1b), and N 1s peak at 399.6 eV (Figure 1c), under the respective narrow scans. Although not shown, the thiol group can also be evident from S 2p binding energy peak at 162.0 eV. Subsequent attachment of GO resulted in the increased C and O intensity seen from the full scan in

Figure 1d, arising predominantly from the GO sheets. In the C 1s narrow scan (Figure 1e), the peaks at 284.6, 286.0 and 288.5 eV were ascribed to the C=C, C-O and C=O of graphene oxide, respectively.¹⁶ Importantly, the peak at 287.6 eV belongs to the O=C-N showing the successful coupling of activated GO by EDC/NHS with cysteine.¹⁷ The weak binding energy peak at 284.8 eV was assigned to the C-S bond of the cysteine self-assembled monolayer on gold surface.¹⁸ The corresponding N 1s narrow scan is as shown in Figure 1f, where amide nitrogen from the coupling reaction of -COOH and -NH₂ is evident at 400.2 eV.¹⁹ The highest binding energy peak in the N 1s spectrum at 402.5 eV can be assigned to the nitrogen of unreacted NHS esters on the surface.²⁰ The attachment of GO on gold surface was further confirmed electrochemically via the cyclic voltammogram of ferricyanide (Figure S3). The electron transfer resistance increases from 950 to 1360 Ω respectively for L-cysteine modified gold electrode and that after GO attachment (Figure S4).

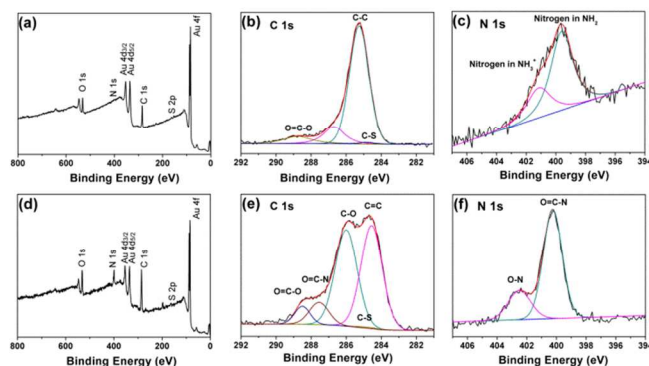


Figure 1. XPS of L-cysteine modified gold electrode: (a) full scan, deconvoluted narrow scans of (b) C 1s binding energy and (c) N 1s binding energy; and GO-modified gold electrode: (d) full scan, deconvoluted narrow scans of (e) C 1s binding energy and (f) N 1s binding energy.

The cyclic voltammetry provides initial qualitative analysis of as-prepared GO-modified electrode before and after adsorption of aqueous metal ions, hereby using Pb²⁺, Cu²⁺ and Hg²⁺ as the model analytes (Figure S5). We confirm that no ion redox peaks could be measured in the NH₄Ac buffer electrolyte (pH 7.0) containing 50 mM KCl prior to the accumulation of heavy metal ions. After accumulation in aliquot containing aqueous metal ions for 10 min (see Figure S6) followed by rinsing with metal-free NH₄Ac buffer, the redox peaks for Pb²⁺, Cu²⁺ and Hg²⁺ appeared at the expected positions of -0.11 V/-0.23 V vs Ag/AgCl,²¹ 0.25 V/0.17 V vs Ag/AgCl,^{19,21b} and 0.55 V/0.51 V vs Ag/AgCl,²² respectively (Figure S5).

Table 1. Detection limits of GO-modified and L-cysteine (prior to GO attachment) modified Au electrode in the sensing of Pb²⁺, Cu²⁺ and Hg²⁺

Electrode	Minimum detection limit (ppb)		
	Pb ²⁺	Cu ²⁺	Hg ²⁺
GO-modified Au	0.4	1.2	0.8
L-cysteine modified Au ^a	20	50	10

^a Calibration plot in Figure S7

For quantitative analysis, the square-wave voltammetry (SWV), which has higher sensitivity compared to the CV technique is employed under the same electrolyte condition as mentioned above. It is well known that the increased sensitivity of SWV arises from

the larger net current (the difference between forward current and reverse current) with very little nonfaradaic and charging currents.²³ Figure 2 shows the calibration curve, measured on the anodic sweep, for (a) Pb²⁺, (b) Cu²⁺ and (c) Hg²⁺, over the GO-modified sensor. Here, regions of linear detection range are evident for all the three metal ions, with detection limits as low as sub-ppb levels were measured for the GO-modified electrode, that is, 0.4 ppb for Pb²⁺, 0.8 ppb for Hg²⁺ and 1.2 ppb for Cu²⁺. These minimum limits are much lower than the guideline values (10 ppb Pb²⁺, 6 ppb Hg²⁺ and 2000 ppb Cu²⁺) for drinking water given by the World Health Organization (WHO),²⁴ and in fact, two orders of magnitudes lower than that of the L-cysteine/gold electrode control, that is, 20 ppb for Pb²⁺, 10 ppb for Hg²⁺ and 50 ppb for Cu²⁺ (Table 1). The ultrahigh sensitivity is attributed to the accumulation of metal ions on the GO surface (shown below), giving rise to improved Faradic to capacitive currents ratio (signal-to-noise, S/N ratio).²⁵ It is interesting to note that the maximum limits of the linear range, 12.8 ppb for Hg²⁺, 51.2 ppb for Pb²⁺ and 200 ppb Cu²⁺, are inversely proportional to the adsorption capacity of GO, suggesting electronic interactions between the adsorbed metal ions when brought to close proximity on GO.²⁶

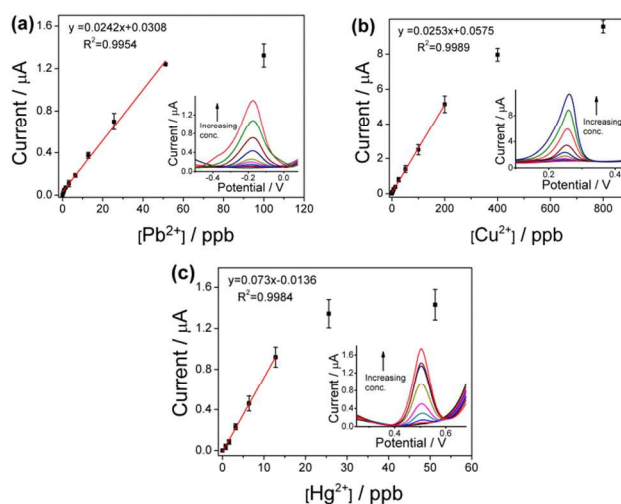


Figure 2. Calibration plots of SWV peak current of (a) Pb²⁺, (b) Cu²⁺ and (c) Hg²⁺ over GO-modified gold electrode. Insets show the corresponding SWV sweep. See Figure S8 for reproducibility measurements for both minimum and maximum linear range detection limits.

The Langmuir adsorption isotherms of Pb²⁺, Cu²⁺ and Hg²⁺ on GO are shown in Figure 3a. The saturation adsorption capacity was estimated 204, 270, 41 mg metal ions/g GO and for Pb²⁺, Hg²⁺ and Cu²⁺, respectively, much higher than other carbon analogues including reduced graphene oxide.²⁷ Previous reports focused either on electrostatic attraction²⁶ or metal coordination¹⁰ between GO and the analyte ions as the possible mode of adsorption. The former appears straightforward given the highly negative zeta potential of GO (Figure 3b) that would readily attract the positive divalent metal ions analyte. However, comparison with rGO, which is also characterized by similar zeta potential profile but with reduced oxygenated moieties, show lower adsorption capacity of 149, 178, 31 mg metal ions/g rGO and for Pb²⁺, Hg²⁺ and Cu²⁺, respectively. Quantification of O:C ratio by XPS revealed three times higher oxygen content for GO (O:C = 2.7) compared to rGO (O:C = 0.09). *Note:* Purification of graphite source prior to Hummers' treatment is necessary to achieve high O:C ratio. However, the adsorption capacities of metal ions on rGO easily exceed above 70% that on GO.

In other words we believe the mixed electrostatic attraction and metal coordination (Figure 3c) may have taken place, the latter is especially dominant on GO. This is further evidenced by the significant aggregation of GO upon addition of metal ions as a result of metal coordination and cross linking of GO sheets (Figure 3d). By comparison, the rGO is only slightly aggregated and the suspension remains stable.

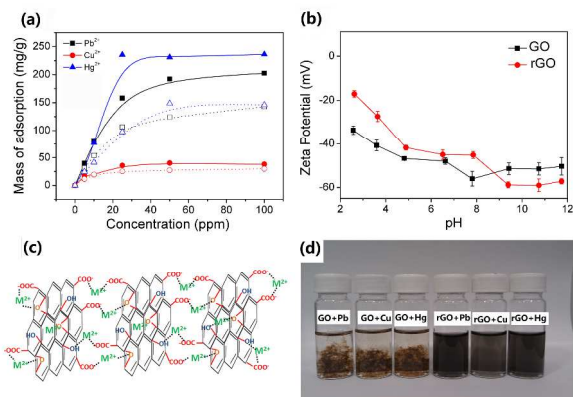


Figure 3. (a) Langmuir adsorption isotherms of Pb²⁺, Cu²⁺ and Hg²⁺ on GO (solid symbols) and rGO (open symbols). (b) Zeta potential of GO and rGO as a function of pH. (c) Illustration of coordination and complexation of metal ions on GO. (d) Photograph showing the aggregation of aqueous GO and rGO induced by the presence of heavy metal ions.

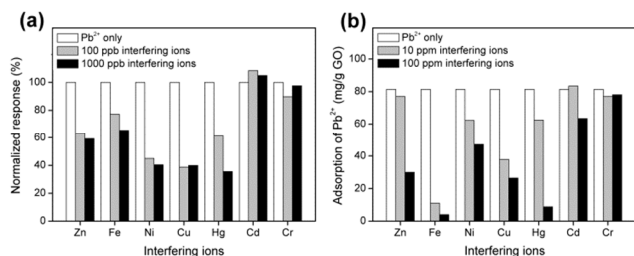


Figure 4. Interference studies in terms of (a) sensing response of 25 ppb Pb²⁺ over GO-modified electrode, and (b) adsorption of 10 ppm Pb²⁺ on GO, in the presence of interfering ions (Zn²⁺, Fe³⁺, Ni²⁺, Cu²⁺, Hg²⁺, Cd²⁺ and Cr⁶⁺).

Using Pb²⁺ as the reference analyte, we further assess the selectivity of the GO-modified electrode. In principle, selective detection requires the covalent attachment of ion-specific antibodies, proteins and polymers²⁸ through the functionalization of the oxygen moieties, which is beyond the scope of the present study. Instead, it is interesting to investigate the selectivity of the “bare” GO as is, which provide further insights on its sensing characteristics. Figure 4a shows the effects of addition of various individual interfering ions, that is, Zn²⁺, Ni²⁺, Fe³⁺, Cd²⁺, Cr⁶⁺, Cu²⁺ and Hg²⁺, during the detection of 25 ppb Pb²⁺. Each test was carried out individually with one interfering ion at low (100 ppb) and high (1000 ppb) concentrations (Figure S9). We found that addition of Zn²⁺, Ni²⁺, Fe³⁺, Cu²⁺ and Hg²⁺ significantly reduced the sensing response of Pb²⁺ at both low and high concentrations of the interfering ions. Essentially, these interfering divalent cations compete with Pb²⁺ ions for the adsorption on GO, through electrostatic attraction and coordination on the oxygenated sites. Along the same analogy, minimal interference was observed in the case of Cr⁶⁺ in the form of chromate (Cr₂O₇²⁻), where there is lack of Cr valance d-orbital for the coordination with the lone pair electrons of oxygen on GO. In fact, the electrostatic repulsion between the Cr₂O₇²⁻ and negatively

charged GO kept the anion separated. The Cd²⁺ has little influence (in fact slightly positive) on the sensing response of Pb²⁺ due to the weak coordination and the similar redox potential as discussed below.²⁹

As competitive adsorption has been identified, Figure 4b shows the net adsorption of 10 ppm Pb²⁺ on GO in the presence of the abovementioned interfering ions. Since direct quantification of adsorption of Pb²⁺ on the GO-modified electrode at ultralow sensing concentration may not be so straightforward, the studies of adsorption interference were conducted in relevance to the Langmuir isotherm. At reference concentration of 10 ppm, adsorbed Pb²⁺ exists as submonolayer on GO (Figure 3a), which in principle allows for sufficient buffer adsorption sites in the presence of low concentration of foreign ions. As shown in Figure 4b, the degree of Pb²⁺ adsorption interference is varied for the different detrimental ions Zn²⁺, Fe³⁺, Ni²⁺, Cu²⁺ and Hg²⁺. Despite assessing in the submonolayer range, the presence of low concentration (10 ppm) of Fe³⁺ significantly reduced the adsorption of Pb²⁺. This is prompted by the stronger coulombic force of attraction between Fe³⁺ and the oxygenated moieties of GO (2.1 times higher compared to Pb²⁺). On the contrary, Zn²⁺ exhibits little adsorption interference at low concentration but at high concentration (100 ppm), the Pb²⁺ adsorption is retarded by more than 60%, implying competitive adsorption when the Langmuir sites become limiting. The same applies to Hg²⁺. Based on the different extent of adsorption interference, it appears that sensing response is not necessarily proportional to the net adsorbed Pb²⁺. For example, much lower sensing response of Pb²⁺ in the presence of Fe³⁺ would be expected relative to Zn²⁺, but this is clearly not the case (Figure 4a). Likewise, the stronger adsorption interference of Cu²⁺ relative to Ni²⁺ was not reflected in the sensing response. The results imply adsorption-induced galvanic interference from the secondary ions during the sensing of Pb²⁺ on GO. Galvanic oxidation of Pb by highly electronegative analytes, i.e., Cu²⁺ and Hg²⁺, resulted in reduced Pb²⁺ stripping signal, more so than in the presence of electropositive interfering ions such as Zn²⁺, Fe³⁺ and Ni²⁺. Since electrostatic repulsion of Cr₂O₇²⁻ kept Cr⁶⁺ away from the GO surface, it did not interfere with the adsorption and sensing response of Pb²⁺. Cd²⁺ shows negligible adsorption interference at low concentration due to the soft acid nature of Cd²⁺ relative to Pb²⁺, and only became obvious at high concentration. Because of the relatively weak interaction, it shows minimal interference to Pb²⁺ sensing.

Finally, the reproducibility of GO-modified electrodes was assessed by comparing the stripping peak current of 50 ppb Pb²⁺, 25 ppb Cu²⁺ and 10 ppb Hg²⁺ using electrodes fabricated on different occasions (n = 5). In all cases, excellent reproducibility of sensing response can be achieved, with relative standard deviations (RSDs) of 2.1% for Pb²⁺, 3.8% for Cu²⁺ and 3.3% for Hg²⁺, revealing the high reproducibility of the electrodes (Figure S10).

Conclusions

In summary, we have showcased a facile fabrication of highly reproducible GO-based electrochemical sensor for ultrasensitive detection of heavy metal ions. The high sensitivity arises from their strong adsorption of these heavy metal ions on the GO, both electrostatically and through metal coordination on oxygenated sites. In this respect, it is more beneficial than the rGO, which lacks the oxygenated group active sites compared to GO (and also simpler in processing, compared to rGO). In general, the showcase device provides a universal platform for which further functionalization with

analyte-specific protein, antibodies and polymers can be achieved through covalent attachment on the oxygenated moieties, for high performance sensors.

Acknowledgements

The authors acknowledge the financial support of Hong Kong UGC through the General Research Fund (CityU 104812) and City University of Hong Kong through Startup Grant (7200252).

Notes and references

¹ *Clean Energy and Nanotechnology (CLEAN) Laboratory, School of Energy and Environment, City University of Hong Kong, Kowloon, Hong Kong S.A.R. E-mail: wyteoh@cityu.edu.hk; Fax: +852-3442 0688; Tel: +852-3442 4627.*

² *Key Laboratory of Pesticide and Chemical Biology of Ministry of Education, College of Chemistry, Central China Normal University, Wuhan, P. R. China.*

† Electronic Supplementary Information (ESI) available: Experimental details on the preparation of GO-modified electrodes, physicochemical characterization and electrochemical measurements, CV and SWV of ferricyanide and heavy metal ions, calibration plots of heavy metal ions, SWV of Pb²⁺ in the presence of interfering ions, and reproducibility measurements of GO-modified electrode.

- (a) A. K. Geim and K. S. Novoselov, *Nat. Mater.*, 2007, **6**, 183-191. (b) J. Wu, W. Pisula and K. Mullen, *Chem. Rev.*, 2007, **107**, 718-747.
- (a) X. S. Li, W. W. Cai, J. H. An, S. Y. Kim, J. H. Nah, D. X. Yang, R. Piner, A. Velamakanni, I. Jung, E. Tutuc, S. K. Banerjee, L. Colombo and R. S. Ruoff, *Science*, 2009, **324**, 1312-1314. (b) D. H. Geng, B. Wu, Y. L. Guo, L. P. Huang, Y. Z. Xue, J. Y. Chen, G. Yu, L. Jiang, W. P. Hu and Y. Q. Liu, *Proc. Natl. Acad. Sci.*, 2012, **109**, 7992-7996.
- (a) S. Park, J. An, I. Jung, R. D. Piner, S. J. An, X. Li, A. Velamakanni and R. S. Ruoff, *Nano Lett.*, 2009, **9**, 1593-1597. (b) S. Some, Y. Kim, Y. Yoon, H. Yoo, S. Lee, Y. Park and H. Lee, *Scientific reports*, 2013, **3**, 1-3.
- (a) S. Park, D. A. Dikin, S. T. Nguyen and R. S. Ruoff, *J. Phys. Chem. C*, 2009, **113**, 15801-15804.
- Z. Liu, J. T. Robinson, X. M. Sun and H. J. Dai, *J. Am. Chem. Soc.*, 2008, **130**, 10876-10877.
- (a) C. H. Liu, Z. Wang, H. X. Jia and Z. P. Li, *Chem. Commun.*, 2011, **47**, 4661-4663.
- W. Gao, L. B. Alemany, L. J. Ci and P. M. Ajayan, *Nat. Chem.*, 2009, **1**, 403-408.
- (a) S. T. Yang, S. Chen, Y. Chang, A. Cao, Y. Liu and H. Wang, *J. Colloid Interface Sci.*, 2011, **359**, 24-29. (b) P. Bradder, S. K. Ling, S. B. Wang and S. M. Liu, *J. Chem. Eng. Data*, 2011, **56**, 138-141.
- (a) C. Xu, X. Wang, L. Yang and Y. Wu, *J. Solid State Chem.*, 2009, **182**, 2486-2490. (b) M. Machida, T. Mochimaru and H. Tatsumoto, *Carbon*, 2006, **44**, 2681-2688.
- (a) S.T. Yang, Y. Chang, H. Wang, G. Liu, S. Chen, Y. Wang, Y. Liu and A. Cao, *J. Colloid Interface Sci.*, 2010, **351**, 122-127. (b) C. Xu, X. Wang, L. C. Yang and Y. P. Wu, *J. Solid State Chem.*, 2009, **182**, 2486-2490.
- M. Mathesh, J. Q. Liu, N. D. Nam, S. K. H. Lam, R. K. Zheng, C. J. Barrow and W. R. Yang, *J. Mater. Chem. C*, 2013, **1**, 3084-3090.
- S. J. Park, K. S. Lee, G. Bozoklu, W. W. Cai, S. T. Nguyen and R. S. Ruoff, *ACS Nano*, 2008, **2**, 572-578.
- W. S. Hummers and R. E. Offeman, *J. Am. Chem. Soc.*, 1958, **80**, 1339.
- (a) H. Yang, S. V. Kershaw, Y. Wang, X. Gong, S. Kalytchuk, A. L. Rogach and W. Y. Teoh, *J. Phys. Chem. C*, 2013, **117**, 20406-20414. (b) D. R. Dreyer, S. J. Park, C. W. Bielawski and R. S. Ruoff, *Chem. Soc. Rev.*, 2010, **39**, 228-240. (c) H. He, J. Klinowski, M. Forster and A. Lurf, *Chem. Phys. Lett.*, 1998, **287**, 53-56.
- (a) L. M. Veca, F. Lu, M. J. Mezziani, L. Cao, P. Zhang, G. Qi, L. Qu, M. Shrestha and Y. P. Sun, *Chem. Commun.*, 2009, 2565-2567. (b) S. Wang, P. J. Chia, L. L. Chua, L. H. Zhao, R. Q. Png, S. Sivaramakrishnan, M. Zhou, R. G. S. Goh, R. H. Friend, A. T. S. Wee and P. K.-H. Ho, *Adv. Mater.*, 2008, **20**, 3440-3446. (c) H. Yang, F. Li, C. Shan, D. Han, Q. Zhang, L. Niu and A. Ivaska, *J. Mater. Chem.*, 2009, **19**, 4632-4638.
- S. Stankovich, D. A. Dikin, R. D. Piner, K. A. Kohlhaas, A. Kleinhammes, Y. Y. Jia, Y. Wu, S. T. Nguyen and R. S. Ruoff, *Carbon*, 2007, **45**, 1558-1565.
- E. Chow, E. L. S. Wong, T. Bocking, Q. T. Nguyen, D. B. Hibbert and J. J. Gooding, *Sens. Actuators B*, 2005, **111**, 540-548.
- G. Doderio, L. De Michieli, O. Cavalleri, R. Rolandi, L. Oliveri, A. Dacca and R. Parodi, *Colloids Surf., A*, 2000, **175**, 121-128
- G. Liu, Q. T. Nguyen, E. Chow, T. Bocking, D. B. Hibbert and J. J. Gooding, *Electroanal.*, 2006, **18**, 1141-1151.
- (a) T. Bocking, M. James, H. G. L. Coster, T. C. Chilcott and K. D. Barrow, *Langmuir*, 2004, **20**, 9227-9235. (b) E. Delamarche, G. Sundarababu, H. Biebuyck, B. Michel, C. Gerber, H. Sigrist, H. Wolf, H. Ringsdorf, N. Xanthopoulos and H. J. Mathieu, *Langmuir*, 1996, **12**, 1997-2006.
- (a) E. Chow, D. B. Hibbert and J. J. Gooding, *Anal Chim Acta*, 2005, **543**, 167-176. (b) N. Kong, J. Q. Liu, Q. S. Kong, R. Wang, C. J. Barrow and W. R. Yang, *Sens. Actuators B*, 2013, **178**, 426-433.
- (a) Z. Q. Zhu, Y. Y. Su, J. Li, D. Li, J. Zhang, S. P. Song, Y. Zhao, G. X. Li and C. H. Fan, *Anal. Chem.*, 2009, **81**, 7660-7666. (b) H. Zhou, X. Wang, P. Yu, X. M. Chen and L. Q. Mao, *Analyst*, 2012, **137**, 305-308.
- (a) J. Osteryoung, J. O'Dea J. Electroanalytical Chemistry; Marcel Dekker: New York, 1986; Vol. 14.
- World Health Organization (WHO), Guidelines for drinking-water quality, Sixty-first meeting, Rome, 10-19 June, 2003, Available from <ftp://ftp.fao.org/es/esn/jecfa/jecfa61sc.pdf>
- (a) J. Cassidy, J. Ghoroghchian, F. Sarfarazi, J. J. Smith and S. Pons, *Electrochim. Acta*, 1986, **31**, 629. (b) K. R. Wehmeyer, M. R. Deakin and R. M. Wightman, *Anal. Chem.*, 1985, **57**, 1913-1916.
- D. Li, M. B. Muller, S. Gilje, R. B. Kaner and G. G. Wallace, *Nat. Nanotechnol.*, 2008, **3**, 101-105.
- (a) M. Imamoglu and O. Tekir, *Desalination* 2008, **228**, 108-113. (b) Y. H. Li, S. Wang, J. Wei, X. Zhang, C. Xu and Z. Luan, *Chem. Phys. Lett.*, 2002, **357**, 263-266. (c) Y. H. Li, J. Ding, Z. Luan, Z. Di, Y. Zhu and C. Xu, *Carbon*, 2003, **41**, 2787-2792. (d) Z. H. Huang, X. Y. Zheng, W. Lv, M. Wang, Q. H. Yang and F. Y. Kang, *Langmuir*, 2011, **27**, 7558-7562.

- 28 (a) D. A. Blake, R. M. Jonesa, R. C. Blake, A. R. Pavlova, I. A. Darwish and H. N. Yu, *Biosensors and Bioelectronics*, 2001, **16**, 799-809. (b) Z. Q. Zhao, X. Chen, Q. Yang, J. H. Liu and X. J. Huang, *Chem. Commun.*, 2012, **48**, 2180-2182.
- 29 E. Chow, D. Ebrahimi, J. J. Gooding and D. B. Hibbert, *Analyst*, 2006, **131**, 1051-1057.